Korean J. Chem. Eng., **30**(2), 295-305 (2013)
DOI: 10.1007/s11814-012-0165-2

Experimental investigation and stability analysis on dense-phase pneumatic conveying of coal and biomass at high pressure

Liang Cai†, Cai Jiaying, Xu Guiling, Xu Pan, Chen Xiaoping, and Zhao Changsui

Key Laboratory of Energy Thermal Conversion and Control of Ministry of Education, School of Energy and Environment, Southeast University, Nanjing 210096, China
(*Received 25 July 2012 • accepted 27 September 2012*)

Abstract−Conveying characteristics and flow stability are very important for design and control of a conveying system at high pressure. The influences of operating parameters and material properties on conveying characteristics were investigated in an experimental test facility with a conveying pressure up to 4 MPa. Wavelet transform and Shannon entropy analysis were applied to analyzing pressure drops through horizontal pipe in order to obtain the stability criterion. Results indicated that the mass flow rate of biomass decreased, while the mass flow rate of pulverized coal increased at first and then decreased with the increase in fluidization velocity. Solid loading ratios for four kinds of powders decreased with the increase in fluidization velocity. Conveying phase diagrams and pressure drops through different test sections of pulverized coal and biomass at high pressure were obtained and analyzed. The influences of coal category, fracture characteristics and particle size on conveying characteristics were determined.

Key words: Pneumatic Conveying, Flow Characteristics, High Pressure, Stability, Shannon Entropy

INTRODUCTION

Pneumatic conveying is widely used to transport solids in the food, minerals and energy process. Such solids include pulverized coal and biomass powder, which are common fuels of the energy industries and essentially serve as the precursor to many chemical products. Good economics would dictate that one always should strive for efficiency with the pneumatic conveying operations to ensure continuous, long-term operation and sufficient cost savings.

Understanding the flow characteristics of pneumatic conveying therefore offers a rich topic for research. Cowell [1] used pulverized coal and surrogate at atmospheric back pressure to compare the two materials' conveying characteristics. Experimental data were used to validate a mathematical model. The similarity of behaviors of the two materials then allowed the model to be applied to the data measured for coal and so generate conveying characteristics at conditions typical of entrained flow. Liang, Chen and Pu [2-4] investigated the effect of pulverized coal properties and operating parameters on flow characteristics at high pressure. Flow regime, stability, state diagram were obtained at different solid loading ratio, conveying velocity and pressure. Pahk [5] applied two different types of plastic pellets to the determination and development of distinguishing flow characteristics. Laouar [6] studied the pressure drop characteristics in pneumatic conveying line at a very low velocity, and obtained a general differential pressure law which proves to be independent of both flow regimes and pipe diameter. Dai and Grace [7] investigated blockage of constrictions by particles in fluid-solid transport using rubber and plastic particles. Experimental results showed that large size, irregular shape, high volumetric concentrations of particles, small constriction dimensions and particle compressibility all increased the likelihood of blockage. Carpinlioglu and Gundogdu [8] investigated the development length of fully suspended flow of solid particles conveyed by air through a horizontal pipeline of circular cross-section using wheat and semolina particles with average diameter 375-825 μm. The development length was correlated as a function of dimensionless parameters d/D, particle loading ratio, Re and Fr. Clementson and Ileleji [9] investigated the bulk density variation of distillers dried grains with soluble when filling and emptying hoppers, simulating the loading of railcars at an ethanol plant. Results showed that there was bulk density and particle size variation as the hoppers were emptied. Segregation that took place while filling the hoppers was amplified during discharge, causing bulk density variation.

The pressure drop signals generated in such systems provide an effective mechanism with which to explore a wide variety of flow behaviors. Many signal analysis methods have been proposed to analyze two-phase flow: example, the power spectrum analysis [10, 11], chaotic analysis [12,13] and wavelet analysis [14,15]. In recent years, Shannon entropy analysis has been applied to the gas-solid two-phase flow. As a state function, Shannon entropy can be applied to predict the degree of uncertainty involved in predicting the output of a probabilistic event. Shannon entropy eliminates the influence of information carrier and data value so as to be used in wide fields. It provides a scientific method to understand the essential state of things. Cho [16] employed Shannon entropy to study heat transfer and temperature difference fluctuations between an immersed heater and the bed in the riser of a three-phase circulating fluidized bed. Zhong [17] applied Shannon entropy to analyze pressure fluctuation and identify the flow regimes in spout-fluid bed. Liang [18-20] applied Shannon entropy to analyze conveying characteristics of pulverized coal at high pressure. Effects of material properties,

†To whom correspondence should be addressed.
E-mail: liangc@seu.edu.cn
‡This work was presented at the 9th China-Korea Workshop on Clean Energy Technology held at Huangshan, China, July, 01-05, 2012.

flow regime and operating parameters on stability were obtained.

However, most reported studies of powder conveying have focused on low pressure and dilute-phase pneumatic conveying. Because of low velocity, high pressure and high solid concentration in transportation at high pressure, the gas-solid two-phase flow becomes very unsteady and complicated. The goal of this study was to explore the flow characteristics in dense-phase pneumatic conveying with two different materials, pulverized coal and biomass powder, by conducting wavelet transform and Shannon entropy analyses. The conveying characteristics and stability of pulverized coal and biomass were investigated. The intention was to provide better understanding of effects of fluidization quality, flow regime and fracture on flow characteristics and stability.

EXPERIMENTAL SYSTEM, MATERIAL PROPERTY AND SIGNAL ANALYSIS

1. Pneumatic Conveying System

The pressurized experimental facility is shown schematically in Fig. 1. High pressure N_2 from the buffer tank was divided into pressurizing gas, fluidizing gas and supplementary gas. The feeding hopper adopted the bottom-fluidization and top-discharge arrangement as shown in Fig. 2. Powder in the feeding hopper was fluidized by fluidizing gas and entered the conveying pipeline through the accelerating section. Supplementary gas was imported to enhance the conveying ability of gas at the outlet of the feeding hopper. To adjust powder moisture content, water through measuring pump was injected into the powder in the conveying pipeline. Pressure in the receiving hopper was controlled by the control valve. Each of the feeding hopper and receiving hopper had a capacity of 0.648 m^3. Conveying pipeline was made of a smooth stainless steel tube with an internal diameter of 10 mm and a length of about 45 m. The length of horizontal pipe and vertical pipe which were used to measure the pressure drop was 100 cm. The 90° mild bends with the radius of 20 cm were about 63 cm in length. The gas volume rates were measured by the metal tube variable-area flow meter, and the fluctuation of solid mass flow rate was gained by the weigh cells. Pressure and pressure drop were measured by semiconductor pressure transducers. Electrical capacitance tomography (ECT) and observation window were used to obtain flow regime and particle density in conveying pipeline as shown in Fig. 3 and Fig. 4. Fig. 3 is the scheme of 8-electrode ECT sensor according to the experiment setup of dense-phase pneumatic conveying at high pressure. The effect of radial electrode on the thick-pipeline sensor was much less than on the conventional sensor. For the purpose of improving capacitance difference and simplifying sensor structure, the designed sen-

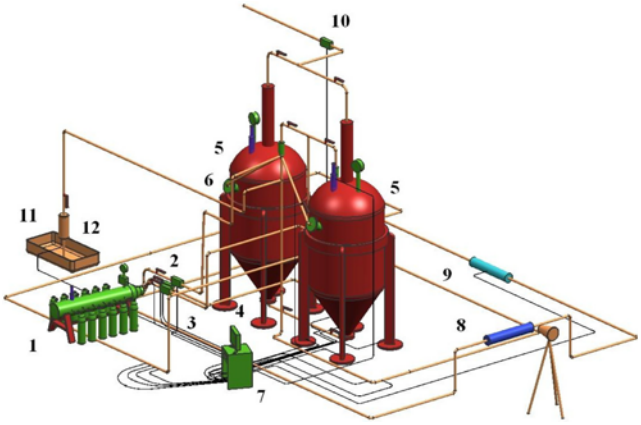

Fig. 1. Schematic diagram of pneumatic conveying system of biomass powder under high pressure.

1. Buffer tank
2. Supplementary gas
3. Pressuring gas
4. Fluidizing gas
5. Hopper
6. Weight cell
7. Data acquisition system
8. Observation window
9. Electrical capacitance tomography system (ECT)
10. Control valve
11. Water
12. Measuring pump

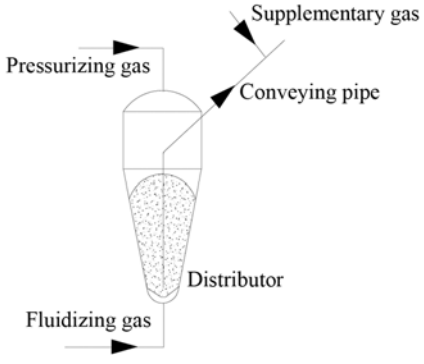

Fig. 2. Diagram of the feeding hopper.

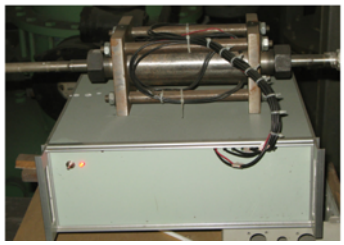

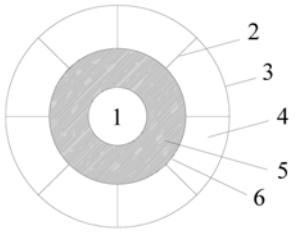

Fig. 3. Small-diameter and high pressure ECT sensor with 8 electrodes.

1. Imaging area
2. Radial electrode
3. Earthed screen
4. Filling layer
5. Insulating pipeline
6. Measurement electrode

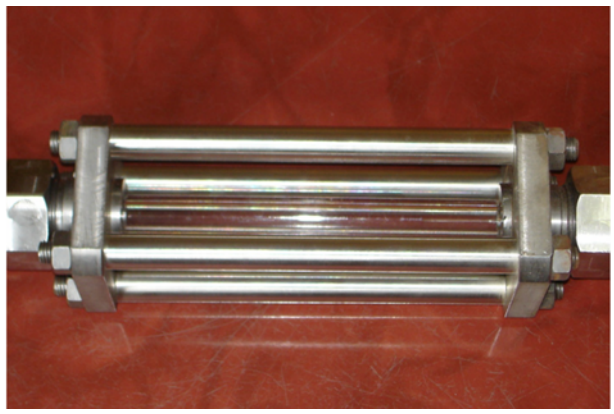

Fig. 4. Observation window.

sor has no radial electrode. The insulating pipeline was made of quartz glass. With a 10 mm inner diameter and a 5 mm thickness, 75 percent of area surrounded the electrodes, which was the high sensitivity area, was occupied by the pipeline wall, as shown in Fig. 3. So this sensor will be less sensitive compared to the conventional one [21]. A high speed video camera photographed the flow regimes through the observation window during the experiments process. To master the fractured characteristics of powder, samples were obtained from the feeding hopper after a period of experiments and mean particle size was measured according to relative standard. Conveying gas was N_2 with the maximum pressure of up to 4.0 MPa. Conveying runs lasted about 20 minutes. Sampling frequencies of load cells, electrostatic sensor, pressure cells and gas flow meters were 1 Hz. Sampling frequencies of pressure drop cells were 200 Hz. The data analysis method is as follows:

1-1. Mass Flow Rate of Powder

The mass of powder conveyed to the receiving hopper is acquired with respect to time. In this way, mass flow rate of powder G is calculated as

$$G = \frac{\Delta W}{\Delta t} \tag{1}$$

where,

ΔW mass of the powder collected in the receiving hopper for a chosen period of time Δt, kg

Δt period of time in which mass of powder ΔW is collected in receiving hopper, h

1-2. Superficial Velocity

As gas is compressible, its velocity changes along the pipeline. Therefore, superficial gas velocity, which will be referred to simply as gas velocity in this paper, can be calculated at gas temperature and average pressure in conveying pipeline

$$U = \frac{Q_a}{A} \tag{2}$$

where,

A cross-sectional area of the pipeline ($A=\pi D^2/4$), m^2

D internal diameter of pipe, m

Q_a gas volume flow rate through the conveying pipeline at gas temperature and average pressure in conveying pipeline, m^3/h

$$Q_a = Q_t \frac{P_s}{P_a}\sqrt{\frac{\rho_s P_b T_s}{\rho_b P_s T_b}} - Q_r \tag{3}$$

P_a average pressure in conveying pipeline, Pa

P_b pressure in the buffer tank, Pa

P_s standard working pressure of flowmeter, 4.1×10^6 Pa

T_b gas temperature in the buffer tank, k

T_s standard working temperature of flowmeter, 293 K

ρ_b gas density in the buffer tank, kg/m^3

ρ_s gas density at standard working condition of flowmeter (4.1×10^6 Pa, 293 K), kg/m^3

Q_t sum of display value of three flowmeters, m^3/h

$$Q_t = Q_f + Q_p + Q_s \tag{4}$$

Q_f display value of flowmeter for fluidizing gas, m^3/h

Q_p display value of flowmeter for pressurizing gas, m^3/h

Q_s display value of flowmeter for supplementary gas, m^3/h

Q_r gas volume flow rate for filling volume occupied by powder conveyed out of the feeding hopper at gas temperature and average pressure in conveying pipeline, m^3/h

$$Q_r = \frac{P_1 G}{P_a \rho_c} \tag{5}$$

P_1 pressure in the feeding hopper, Pa

ρ_c powder density, kg/m^3

1-3. Solid Loading Ratio

There are a few different ways to express the concentration of powder in the gas-solid two-phase flow. One of the most common is the ratio of mass flow rate to gas volume flow rates, called solid loading ratio, which can be easily calculated as

$$\mu = \frac{G}{Q_a} \tag{6}$$

2. Material Property

Biomass powder and pulverized coal were used to investigate conveying characteristics at high pressure as shown in Table 1. The external moisture content was measured using procedures set out in china measuring standards of powder. This involved heating a known mass of powder in a pre-heated oven at a temperature between 45 °C and 50 °C for a minimum of 2 hours; the moisture content of the powder samples was calculated by recording the weight loss occurring during drying of the powder samples. Because of high moisture content, irregular shape and sizes, and low bulk density, biomass was very difficult to handle, transport, store, and use in its original form. Biomass samples were pretreated in this study. Two kinds of biomass powders had similar apparent density, external moisture content but different mean particle size as shown in Table 1. Micrographs of biomasses using scan electron microscope are presented in Fig. 5. Particles of biomass powders had poor degree of sphericity, which was soft (not rigid) and more pliable. Two coal samples used for comparative test are from the same parent coal. The major difference between two coal samples was mean particle size. The initial moisture content in coals was different because of coal categories and handling processes. The external moisture content

Table 1. Material property of pulverized coal and biomass powder

	Real density (kg/m^3)	Bulk density (kg/m^3)	External moisture content (%)	Mean particle size (μm)
Biomass with small particle size	1480	464	0	120
Biomass with large particle size	1480	430	0	260
Coal with small particle size	1490	653	3.4	52
Coal with large particle size	1470	648	0.4	300

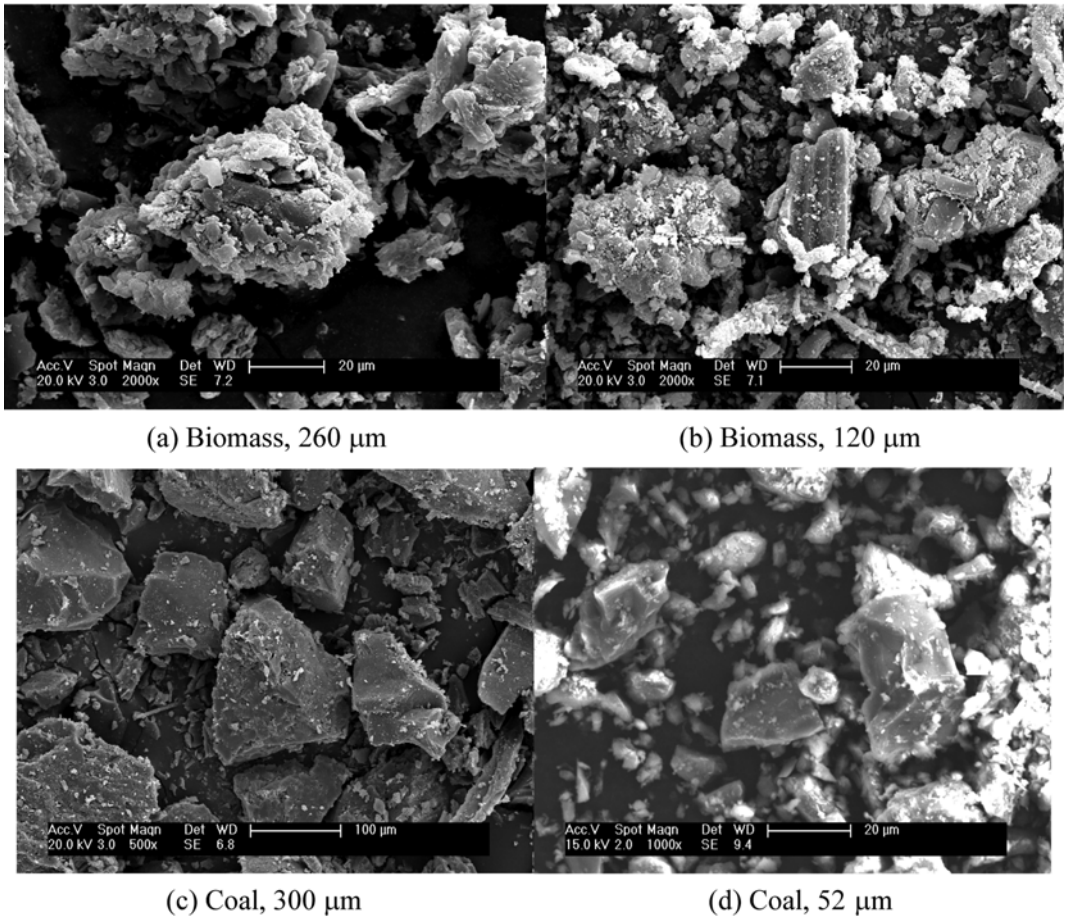

Fig. 5. Micrographs of powders using SEM.

and the total moisture content of pulverized coals are measured in Table 1. To study the effect of particle shape on conveying characteristics, SEM pictures of two types of pulverized coal are shown in Fig. 5. It indicated that coal particle sizes have good sphericity.

3. Signal Analysis

Wavelet analysis and Shannon entropy were used to extract characteristic parameters to represent flow stability in this paper. The signals were denoised by the wavelet analysis and then characteristic parameters were abstracted using Shannon analysis. In wavelet analysis, dilating or contracting the chosen analyzing wavelet before convolving it with the signal accomplishes scale decomposition. The original signals can be resolved into multi-resolution signals with different frequency bands. It is shown that the raw data can be decomposed into different scale signals and detail signals (wavelet transform), and the original signal may be reconstructed from the information contained in the last scale signal and detail signals. Wavelet analysis can be used to eliminate noise, but it is difficult to extract characteristic parameters. Shannon entropy can be utilized to predict the degree of uncertainty involved in predicting the output of a probabilistic event. Shannon entropy eliminates the influence of information carrier and data value so as to be used in wide fields. If signals include in noise, characteristic parameters which are extracted by Shannon entropy do not necessarily represent flow regime, stability and so on. So in order to obtain characteristic parameters of pneumatic conveying, signals must eliminate noise at first and then extract characteristic parameters. This is because characteristic information of pressure drop signal in pneumatic conveying is mainly distributed in the low frequency. To obtain the stability criterion, wavelet transform and Shannon entropy analysis offer an attractive method to analyze the pressure drop signal. Since the pressure drop signal represents the sum of flow characteristic, stability and so on, the wavelet transform enables one to decompose this signal using a mother wavelet with dilation and translation operations. Thus the noise and interference signal in pressure drop is rejected and wavelet transform yielding wavelet coefficients after filtering reconstructed the new signal. Thus the Shannon entropy was utilized to abstract characteristic parameters to identify flow stability.

Discrete wavelet transform is a transformation of information from a fine scale to a coarser scale by extracting information that describes the fine scale variability (the detail coefficients or wavelet coefficients) and the coarser scale smoothness (the smooth coefficients or mother-function coefficients)

According to:

$$\{D_j\}=[G]\{S_{j+1}\};\ \{S_j\}=[H]\{S_{j+1}\} \tag{7}$$

where S represents mother-function coefficients, D represents wavelet coefficients, j is the wavelet level, and H and G are the convolution matrices based on the wavelet basis function. High values of j signify finer scales of information. The complete wavelet transform is a process that recursively applies Eq. (7) from the finest to the

coarsest wavelet level (scale). This describes a scale-by-scale extraction of the variability information at each scale. The mother function coefficients generated at each scale are used for the extraction in the next coarser scale. The inverse discrete wavelet transform is similarly implemented via a recursive recombination of the smooth and detail information from the coarsest to finest wavelet level (scale):

$$\{S_{j+1}\}=[H]^T\{S_j\}+[G]^T\{D_j\} \quad (8)$$

Where H^T and G^T indicate the transpose of H and G matrices, respectively.

The matrices H and G are created from the coefficients of the basis functions, and represent the convolution of the basis function with the data.

In this study, wavelet coefficients of a signal are computed based on the discrete wavelet transform (Eq. (7)). Because noise is mainly distributed at high frequency of signals, the wavelet coefficients of noise are filtered. Inverse wavelet transform (Eq. (8)) is applied to the wavelet coefficients at each wavelet level, and the components of signal are obtained after wavelets denoise.

In 1948, Shannon first defined the concept of Shannon entropy and used a formula to measure information content. In the developing process, it associated with entropy of physics. As a state function, Shannon entropy can be used to predict the degree of uncertainty involved in predicting the output of a probabilistic event. That is, if one predicts the outcome exactly before it happens, the probability will be a maximum value and, as a result, the Shannon entropy will be a minimum value. If one is absolutely able to predict the outcomes of an event, the Shannon entropy will be zero. Shannon entropy eliminates the influence of information carrier and data value so as to be used in wide fields. It provides a scientific method to understand the essential state of things.

The discrete new signal of X(t) after wavelet denoising can be written as $X=\{x_1, x_2, \cdots, x_n\}$. Values of X may be divided into bins, each with a range in X(t), and denoted by values $X_1, X_2, \cdots, X_n$. Then, the probability of any value of X is $P(X_i)=X_i/n$. Hence, a set of probability $P(X_1), P(X_2), \cdots, P(X_n)$, can be created from the original data set. The Shannon entropy of any pressure drop time series in the pneumatic conveying can be defined as

$$S(X)=-\sum_{i=1}^{n}P(x_i)\log_b P(x_i) \quad (9)$$

Where, n is the length of time series signal, $P(x_i)$ is the probability of every component in the signal, satisfying the constraint $\sum_{i=1}^{n}P(x_i)=1$. When b=2, e and 10, the unit of S is bit, nat and hart, respectively. In this paper, the value of b is e. Shannon entropy can be seen when there is more disorder in a system and the information entropy is larger. Shannon entropy in pneumatic conveying reflects the flow stability. A pressure drop with 20000 data points was chosen to reveal conveying stability using wavelet transform and Shannon entropy analysis in this paper.

RESULTS AND DISCUSSION

1. Effect of Fluidization Velocity on Conveying Characteristics and Flow Stability

Fluidizing gas was used to fluidize powder and its flow rate determined the fluidization quality of powder particles in the feeding hopper. However, little work has been done to understand the fluidization characteristics of powder particles at high pressure. It generally appeared to be assumed that the design and operation of equipment involving powder materials could be based on conventional fluidization knowledge and methodologies. To investigate the effect of fluidization velocity on conveying characteristics of biomass powder and pulverized coal, conveying experiments of different fluidization velocity were carried out. The superficial velocity of the horizontal cross-section of the discharge pipe inlet in a feeding hopper was defined as fluidization velocity U_f. Critical fluidization velocity U_{mf} of the particle can be calculated by the following equation:

Table 2. Critical fluidization velocity and Critical fluidization number of four kinds of powders

	Critical fluidization velocity (m/s)	Critical fluidization number
Biomass with smaller particle size	0.0078	1.9
Biomass with larger particle size	0.0286	2.0
Coal with smaller particle size	0.0015	3.0
Coal with larger particle size	0.0347	3.1

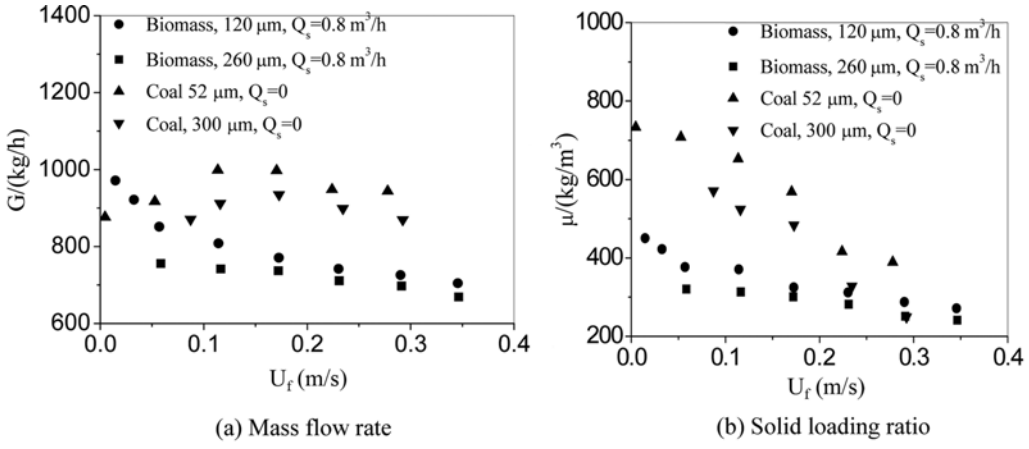

Fig. 6. Effect of fluidizing velocity on flow characteristics (P1=3.60-3.70 MPa, P2=2.80 MPa).

$$U_{mf}=\frac{Re_{mf}\mu_{gas}}{d\rho_{gas}} \quad (10)$$

Where Re_{mf} is the critical Reynolds number, μ_{gas} is the viscosity of conveying gas, d is the mean particle size of powder, ρ_{gas} is the density of conveying gas. The critical fluidization velocity calculated according to Eq. (10) and critical fluidization numbers for the four kinds of powders are listed in Table 2. Effect of fluidization velocity on flow characteristics is presented in Fig. 6. As shown in Fig. 6(a), the mass flow rate of biomass decreased, while the mass flow rate of pulverized coal increased at first and then decreased with the increase in fluidization velocity. As fluidizing number was below 1.9, fluidization quality of powder in feeding hopper was worse and it was difficult to feed powder into the conveying pipeline. Arching and blockage were often present in the conveying process. With the increase in fluidization velocity, flow ability of powder was enhanced. Biomass with small particle size can be conveyed as fluidizing number was over 1.9. Biomass with larger particle size can be conveyed until the fluidizing number is over 2.0. While for the pulverized coal, results were significantly different. Because of good sphericity and high apparent density, pulverized coal was more difficult to fluidize. Pulverized coal with smaller particle size can be conveyed until fluidizing number is above 3.0. From the Table 2, the results show that critical fluidization number of biomass was less than that of coal. Thus biomass particle was easier to fluidize than coal particle in the feeding hopper. At this time, the solid loading ratio of fluidized area in the feeding hopper was larger. Therefore, the mass flow rate of biomass in conveying pipeline was larger as shown in Fig. 6(a). As fluidization velocity continued to rise, decrease in solid loading ratio of fluidized area in the feeding hopper led to reduction in mass flow rate. So mass flow rate of biomass decreased with the increase in fluidization velocity. Pulverized coal was partially fluidized and flowability was worse as fluidizing number was less than 3.0. Thus it was difficult for pulverized coal to enter into the conveying pipeline and mass flow rate was less. With the increase in fluidization velocity, solid loading ratio in feeding hopper decreased and gas-solid two-phase flow was easier to be fed into the conveying pipeline. In this stage, the mass flow rate of pulverized coal increased with the increase in fluidization velocity. When fluidization velocity continued to rise, gas-solid two-phase flow became dilute and discharge rate of pulverized coal decreased. So the mass flow rate of pulverized coal increased at first and then decreased with the increase in fluidization velocity. All of those differences were induced by the material properties of biomass and pulverized coal. Since solid loading ratio in feeding hopper always decreased with the increase in fluidization velocity, solid loading ratio decreased in conveying pipeline as shown in Fig. 6(b). Because more energy was required to convey larger size particles for the same conveying conditions, mass flow rate and solid loading ratio with smaller particle size were larger than that with larger particle size for same material categories [5,22].

The pressure drop signals generated in such systems provided an effective mechanism with which to explore a wide variety of flow behaviors. To obtain stability criterion of pneumatic conveying, characteristic parameters in pressure drop through horizontal pipe was extracted using wavelet transform and Shannon entropy analysis. The effect of fluidization velocity on Shannon entropy is shown in Fig. 7. Shannon entropy of pressure drop through horizontal pipe decreased with the increase in fluidization velocity. As fluidization velocity was less, solid loading ratio was the highest in the feeding hopper and the flowability of gas-solid two-phase flow of pulverized coal was worse, which resulted in instability of mass flow rate and fluctuation of pressure drop as shown in Fig. 8. The value of Shannon entropy was larger than 8 nats in Fig. 7, while mass flow rates and pressure drops through different test sections for biomass powders were stable as shown in Fig. 9. So the conveying process showed good stability at lower fluidization velocity. With the increase in fluidization velocity, conveying flowability increased and Shannon entropy decreased. To the pulverized coal, solid loading ratio was below 500 kg/m^3 and conveying system showed the excellent work state when fluidization velocity was more than 0.18 m/s. Shannon entropy decreased and was below 8 nats as shown in Fig. 7. Hence, flow stability improved gradually with increase in fluidiza-

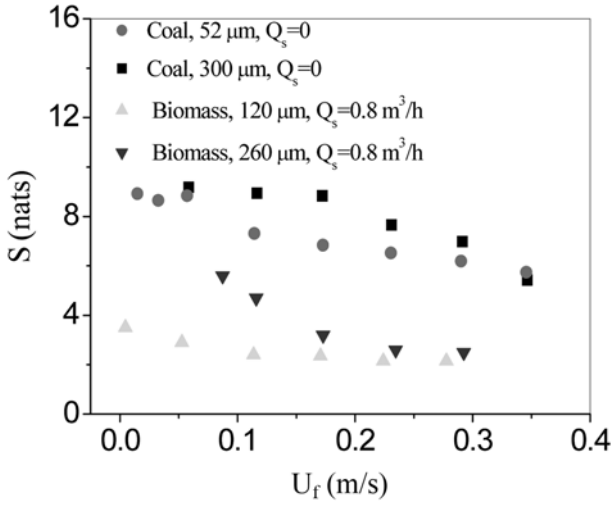

Fig. 7. Effect of fluidizing velocity on Shannon entropy.

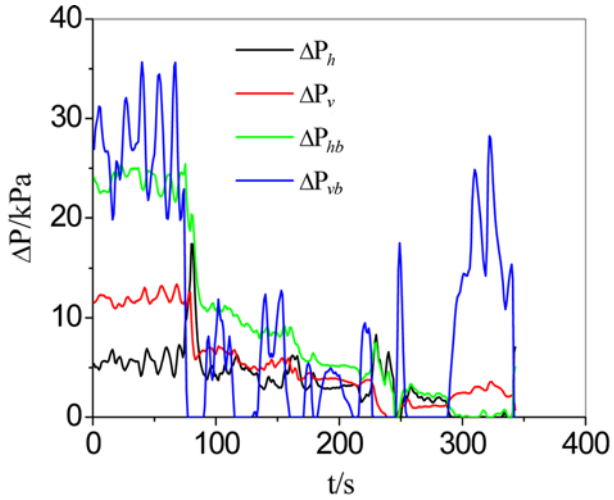

Fig. 8. Time series of pressure drop with arching in the feeding hopper (ΔP_h - Pressure drop through horizontal pipe; ΔP_v - Pressure drop through vertical pipe; ΔP_{hb} - Pressure drop through horizontal bend; ΔP_{vb} - Pressure drop through vertical bend) (P_1=3.60-3.70 MPa, P_2=2.80 MPa, Q_s=0 m^3/h, d_p=300 μm).

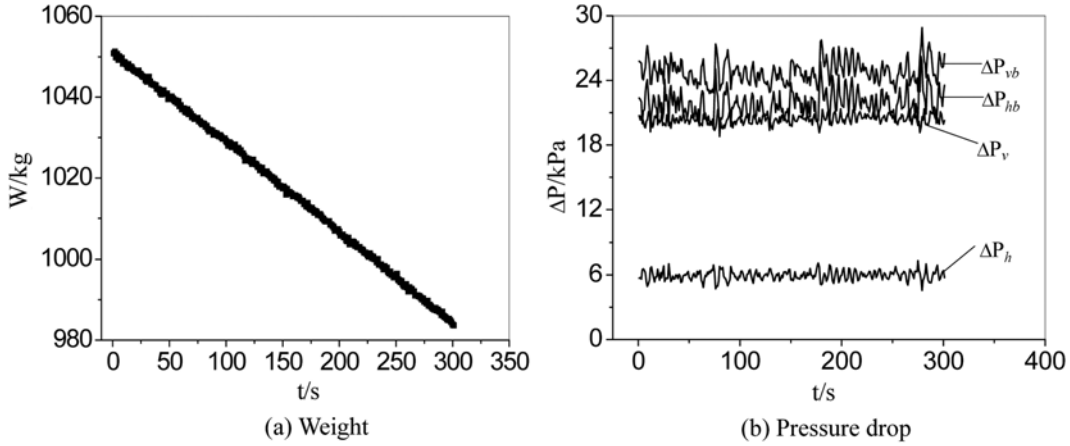

Fig. 9. Conveying stability of biomass as U_f=0.05 m/s (P_1=3.60-3.70 MPa, P_2=2.80 MPa, Q_s=0.8 m^3/h, d_p=120 μm).

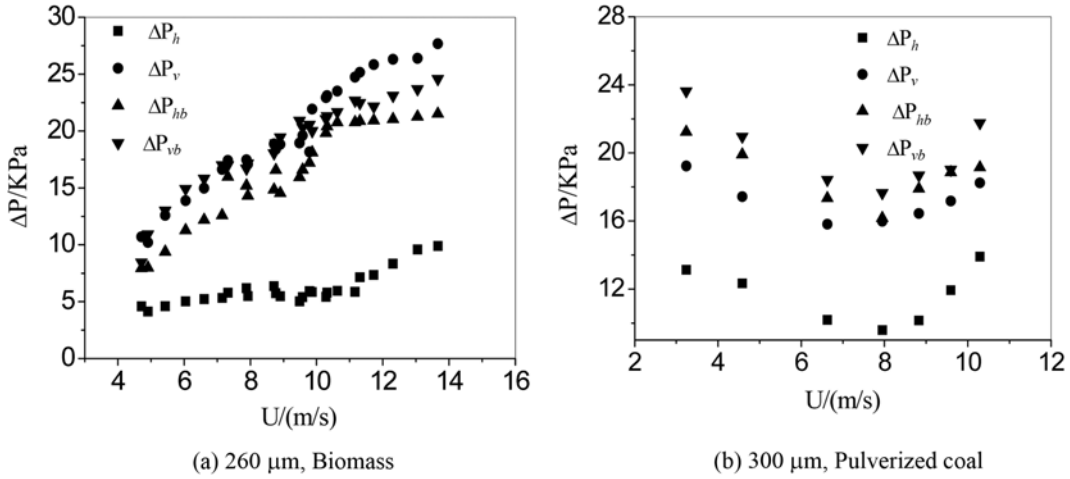

Fig. 10. State diagram of pulverized coal and biomass (P_1=3.60-3.70 MPa, P_2=2.80 MPa).

tion velocity, which was induced by flowability of pulverized coal in the feeding hopper, solid loading ratio and so on. To the biomass powder, fluidization quality was enhanced and gas-solid two-phase flow showed good flowability with the increase in fluidization velocity. Flow stability increased and Shannon entropy decreased as shown in Fig. 7. Conveying process of biomass showed good stability at different fluidization velocity. Thus conveying flowability increased and Shannon entropy decreased with the increase in fluidization velocity.

2. Effect of Flow Regime on Conveying Characteristics and Flow Stability

Fluidization velocity, pressures in feeding hopper and receiving hopper were the same in the entire experiment process. In the state diagram, the mass flow rate remained constant at different conveying velocity. Thus solid loading ratio decreased with the increase in conveying velocity (3 m/s<U<15 m/s). The state diagram of conveying is plotted in Fig. 10. Results show that pressure drops through different test sections for biomass increased with the increase in conveying velocity in Fig. 10(a). Whereas, pressure drops through different test sections for pulverized coal decreased at first and then increased with the increase in conveying velocity Fig. 10(b). Biomass particles tended to concentrate in the low portions of straight

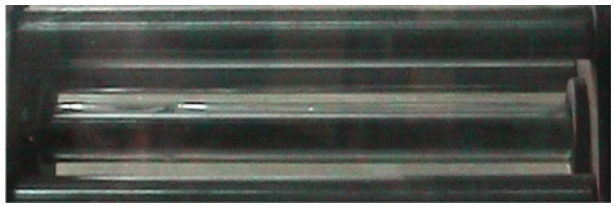

Fig. 11. Picture of flow regime of biomass.

horizontal pipe and showed suspended flow at low flow velocities as shown Fig. 11. With increase in conveying velocity, solid loading ratio decreased and homogeneous flow appeared in the conveying process. Pressure drops through different test sections increased as conveying velocity rose in Fig. 10(a). While for pulverized coal, flow characteristics were significantly different to biomass. It indicated that pressure drops through different test sections decreased at first and then increased with the increase in conveying velocity in Fig. 10(b). The flow was quite dilute and pulverized coal was conveyed homogeneously when the conveying velocity was very high. Pressure drop was attributed mainly by gas movement. Here particles were carried in the gas while bouncing frequently

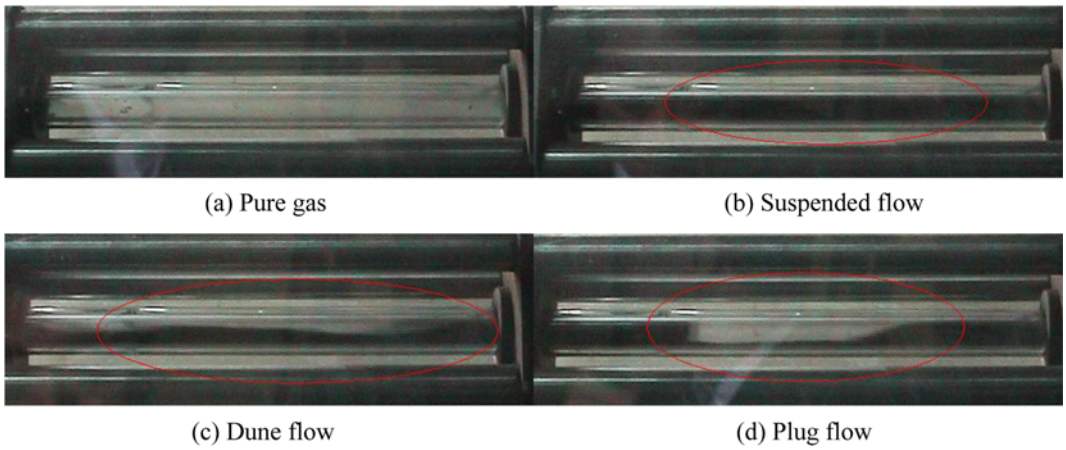

Fig. 12. Flow regimes of pulverized coal at different conveying velocity.

against the pipe wall and conveying presented the suspended flow as shown in Fig. 12(b). As the superficial velocity decreased, the particle concentration increased. The pressure drop of gas phase decreased and that of solid phase rose. When the increment of the pressure drop caused by the solid phase equaled the decrement in pressure drop caused by the gas phase, pressure drop appeared to be the minimum. This conveying velocity is called the economic velocity. Near the economic velocity, a suspended phase and a settled layer of pulverized coal were frequently observed. As conveying velocity was greater than economic velocity, the flow regime is typically described as dilute flow. When conveying velocity was lower than economic velocity, dunes or clusters can be seen riding on a settled layer of pulverized coal as shown in Fig. 12(c). A further reduction in the gas velocity would lead to a region typically characterized by unstable flow. At even lower gas velocities the material may flow as plugs as shown in Fig. 12(d). Therefore, biomass powder presented suspended flow at different conveying velocity. Pulverized coal revealed different flow regime as shown in Fig. 12. Differences of state phase between pulverized coal and biomass were largely the result of different conveying regime.

The effect of flow regime on Shannon entropy is presented in Fig. 13. Results showed that Shannon entropy for biomass decreased

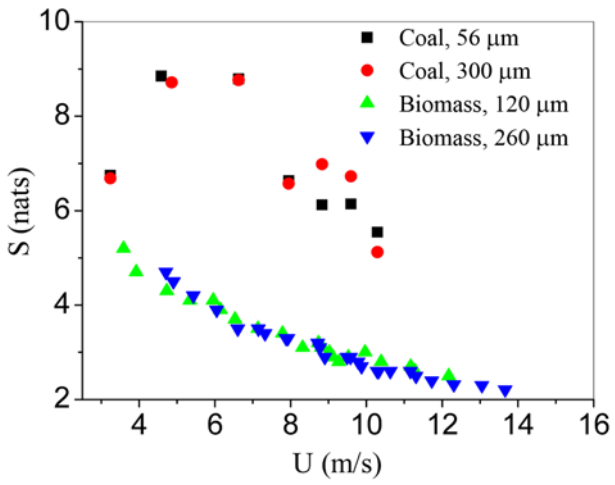

Fig. 13. Shannon entropy at different conveying velocity.

while Shannon entropy for pulverized coal increased at first and then decreased with the increase in conveying velocity. As conveying velocity was lower, flocculated flow for biomass powder was presented in the conveying process. Density of biomass powder showed a great difference in cross-section of conveying pipeline. Biomass particles in the top of conveying pipeline were fewer and particles were carried by the high-speed gas. Powder friction between the layers resulted in flow fluctuation in the conveying process. Thus the Shannon entropy was greater because of conveying fluctuation as shown in Fig. 13. With the increase in conveying velocity, solid loading ratio decreased and flow regime presented homogeneous flow. Stability of gas-solid two-phase flow was enhanced and Shannon entropy decreased. While the Shannon entropy for biomass was less than 6 nats in the whole experiment, the conveying process maintained good stability at different conveying velocity (3 m/s<U<14 m/s). While to the pulverized coal, flow characteristics were different. Towards the right end of the curve in Fig. 10(b), lower solid-gas ratio reduced inter-particle contact and high gas velocities enabled the particles to be carried in suspension, yielding an extremely stable conveying state as shown in Fig. 12(b). Erosion and particle attrition of coal particle were intense in this state. Shannon entropy was less than 7 nats, but pressure drop was greater as conveying regime showed suspension flow Fig. 10(b). As the gas velocity was reduced, forces leading to the suspension of the particles began to diminish and a portion of the coal particles fell out of suspension to form a sliding or rolling layer on the bottom of the conveying line. This type of conveying represented a metastable state. Pressure drop decreased and Shannon entropy increased. Good stability still showed in the conveying process. With the decrease in superficial velocity, conveying entered into an unstable flow regime characterized by the formation and decay of dense clusters or dunes of pulverized coal as shown in Fig. 12(c). Such phenomena as collapsing of a dune to provide the necessary reduction of conveying area to permit dilute phase flow or its combination with another dune to produce the plug often appeared in this regime. Erratic flow conditions caused drastic fluctuations in the pressure drop. Thus pressure drop increase and decrease in conveying stability led to increase of Shannon entropy. Further to the left of the unstable zone there existed another stable conveying region for pulverized coal where powder material was transported as discontinuous, quasi-

discrete plugs in Fig. 12(d). In this region, gas velocity was small enough so that the drag forces necessary to carry the material as individual particle were not produced. Consequently, particles remained close to each other, causing the system to behave as a packed bed, where gas was squeezed through narrow channels producing a high pressure drop required to move plugs of material. For such discrete plugs to exist, the pressure drop must increase quickly to compensate for the large amount of wall friction that must be overcome. Thus, pressure drops through different test sections increased with the increase in conveying velocity in plug region. Because conveying was the periodical movement steadily in plug flow, Shannon entropy was less than 7 nats.

3. Fracture Characteristics and Flow Stability of Biomass and Coal

The properties of powder particles are sufficiently unique that blockage, fracture and arching of biomass and pulverized coal particles are not fully understood. On the whole, the flowability of biomass was worse than that of pulverized coal. Blockage often occurred during the pneumatic conveying process for biomass. Start-up conveying velocity of biomass must be much higher than that of pulverized coal, normally over 8 m/s; otherwise, blockage would happen easily. After an experiment run is started successfully, the conveying parameters can be adjusted according to the experimental requirement. Pulverized coal can be conveyed as conveying velocity was more than 3 m/s. Because of pliability, flexibility and compressibility of biomass, friction between biomass particle and pipe wall was great. Conveying gas was very easy to penetrate the biomass powder. At the start-up state, solid loading ratio was greater and conveying gas penetrated the biomass powder into the receiving hopper. So biomass particles with lower velocity concentrated in the low portions of conveying pipe. Such local increases in particle concentration may cause already-dispersed biomass to reflocculate. Thus, biomass particles revealed agglomeration in the subsequent channel system and forming section, which resulted in blockage. While pulverized coal had great bulk density, good sphericity and flowability, conveying gas was difficult to penetrate the pulverized coal and high pressure gas had to push the coal layer ahead. Thus pulverized coal was easier to convey than biomass powder in start-up stage.

In conveying experiment, the biomass and coal powder were used circularly. Mean particle sizes (d) of biomasses decreased while Shannon entropy increased with the increase in conveying number (n) in Fig. 14 and Fig. 15. As biomass powder was initially used in the conveying experiment, the conveying process showed good stability and Shannon entropy was less as shown in Fig. 15. This was

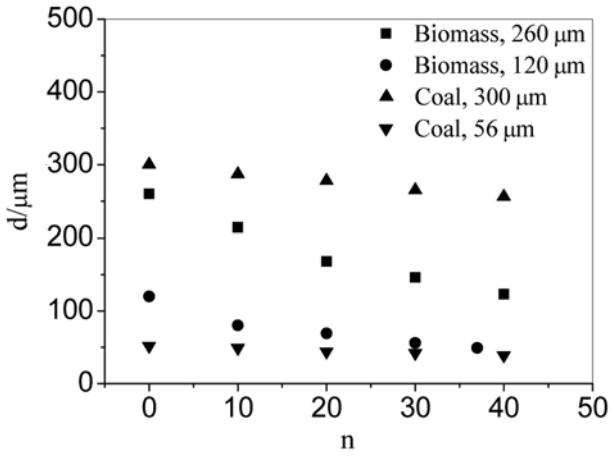

Fig. 14. Attrition characteristic of biomass particle (d is the mean particle size, n is the number of conveying runs).

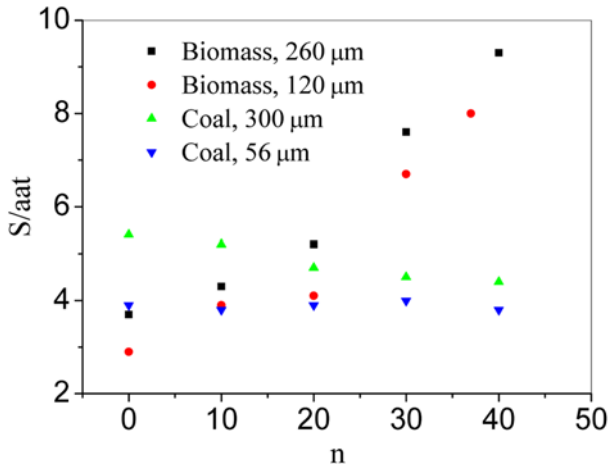

Fig. 15. Effect of conveying number on Shannon entropy.

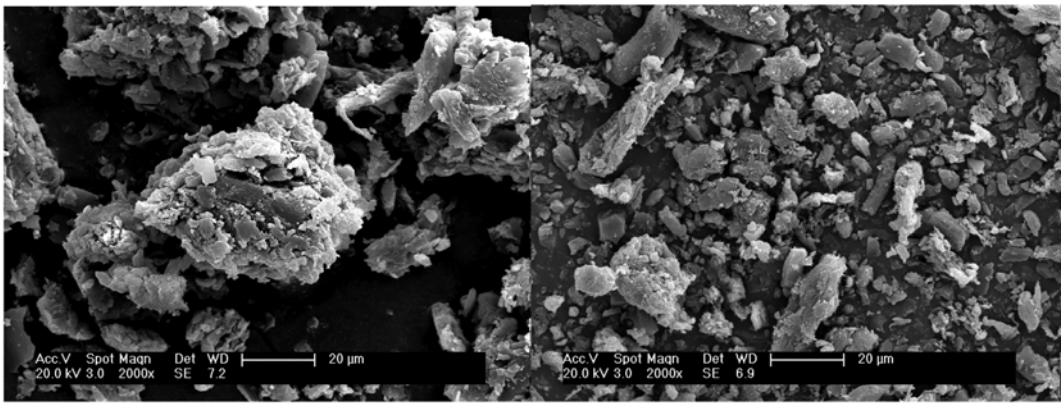

(a) Sample before experiment (b) Sample after experiment

Fig. 16. Micrographs of biomass particle with large size.

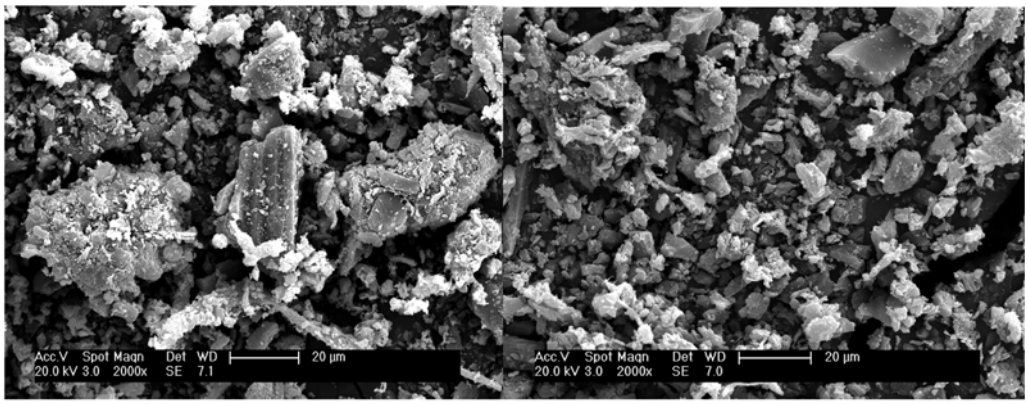

(a) Sample before experiment (b) Sample after experiment

Fig. 17. Micrographs of biomass particle with small size.

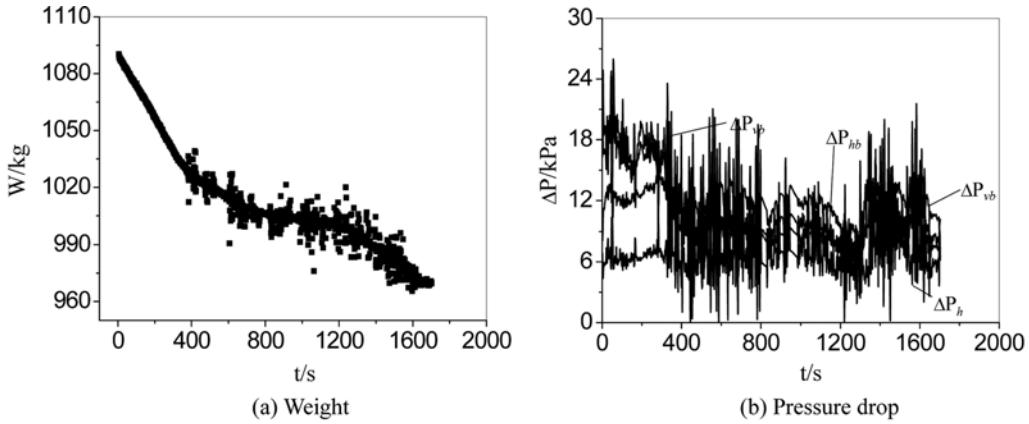

(a) Weight (b) Pressure drop

Fig. 18. Arching characteristic of biomass in conveying process.

because the biomass particles were soft and more pliable as shown in Fig. 16(a) and Fig. 17(a). In the conveying process, collision and friction between particles and wall led to fracture of biomass particles. With the increase in conveying number, the number of fine particles rose and the degree of particle sphericity became worse in Fig. 16(b) and Fig. 17(b). The flowability decreased and Shannon entropy increased as shown in Fig. 15. Biomass sample had to be changed to a new sample after about 40 runs were achieved. Otherwise, conveying could not continue due to the bridging in the feeding hopper as shown in Fig. 18. While for the pulverized coal, the fracture characteristics of particles were different from the biomass particles. Particle size and Shannon entropy of pulverized coal with the larger size decreased, but particle size and Shannon entropy of pulverized coal with smaller size almost remained constant with the increase in conveying number as shown in Fig. 14 and Fig. 15. In the whole conveying experiments for pulverized coal, the conveying showed good stability. Biomass particles showed good sphericity before the conveying experiment began. With the increase in conveying runs, biomass fractured gradually and revealed needle-like or columnar particles. Thus, flowability and fluidization of biomass became worse gradually in the feeding hopper because of high cohesion forces among the particles and wall. Arching often occurred and conveying could not continue. Thus, flowability and stability of biomass decreased with the increase in conveying time. Biomass powder had to be changed to new sample after a certain runs. Otherwise, conveying could not continue due to the bridging in the feeding hopper. While coal particles were rigid and had good flowability, the change of mean particle size was very small as shown in Fig. 14. With the increase in conveying number, flow stability of pulverized coal with larger particle size rose and Shannon entropy decreased. Because the particle size of pulverized coal with smaller particle size almost remained constant, flow stability and Shannon entropy remained unchanged. Pulverized coal did not experience arching because of good sphericity and flowability.

CONCLUSIONS

Influences of fluidization velocity, flow regime, material properties, etc., on conveying characteristics and flow stability of pulverized coal and biomass were investigated in dense-phase conveying system at high pressure. Conveying differences of biomass and pulverized coal were obtained and results are as follows:

(1) With the increase in fluidization velocity, mass flow rate and solid loading ratio of biomass decreased but mass flow rate of pulverized coal increased at first and then decreased. Biomasses could be conveyed successfully as fluidizing number was more than 1.9 but pulverized coal could only be conveyed until fluidizing number was above 3.0. Mass flow rate and solid loading ratio with smaller particle

size were larger than that with larger particle size for the same material category. With the increase in fluidization velocity, conveying flowability increased and Shannon entropy decreased.

(2) In the state diagram, pressure drops for biomass increased while pressure drops for pulverized coal decreased at first and then increased with the increase in conveying velocity. Two types of suspension flow regimes for biomass were identified: flocculated flow and homogeneous flow. Pulverized coal revealed different flow regimes: plug flow, dune flow and suspended flow with the increase in conveying velocity. With the increase in conveying velocity, Shannon entropy for biomass decreased, while Shannon entropy for pulverized coal increased at first and then decreased.

(3) The flowability of biomass was worse and blockage often occurred during pneumatic conveying process. Start-up conveying velocity of biomass must be higher than 8 m/s; otherwise, the blockage will occur easily. Pulverized coal can be conveyed as conveying velocity is more than 3 m/s. Mean particle sizes of two kinds of biomass decreased but mean particle sizes of pulverized coals were almost constant with the increase in conveying number. Biomass powder had to be changed to a new sample after certain runs in the tests. Otherwise, conveying could not continue due to the bridging because of fracture. With the increase in conveying number, flow stability of pulverized coal with larger particle size rose and Shannon entropy decreased. Because particle size of pulverized coal with smaller particle size almost remained constant, flow stability and Shannon entropy showed unchanged. Conveying stability decreased and Shannon entropy increased with the increase in conveying number.

ACKNOWLEDGEMENTS

We acknowledge the support of the Special Funds of National Key Basic Research and Development Program of China (2010CB 227002), National Natural Science Foundation of China (50906011) and Major Scientific Research Fund of Southeast University.

NOMENCLATURE

A : cross-sectional area of the pipeline ($A=\pi D^2/4$) [m^2]
D : inside diameter of pipe [m]
G : mass flow rate of pulverized coal [kg/h]
M : external moisture content of coal [%]
P_1 : pressure in the feeding hopper [MPa]
P_2 : pressure in the receiving hopper [MPa]
P_a : average pressure in conveying pipeline [Pa]
P_b : pressure in the buffer tank [Pa]
P_s : standard working pressure of flowmeter, 4.1×10^6 Pa
ΔP : pressure drop through test sections [kPa]
ΔP_h : pressure drop through horizontal pipe section [kPa]
ΔP_{hb} : pressure drop through horizontal bend [kPa]
ΔP_v : pressure drop through vertical pipe section [kPa]
ΔP_{vb} : pressure drop through vertical bend [kPa]
Q_a : gas volume flow rate through the conveying pipeline at gas temperature and average pressure in conveying pipeline [m^3/h]
Q_f : fluidizing gas flow rate [m^3/h]
Q_p : display value of flowmeter for pressurizing gas [m^3/h]
Q_r : gas volume flow rate for filling volume occupied by powder conveyed out of the feeding hopper at gas temperature and average pressure in conveying pipeline [m^3/h]
Q_s : supplementary gas flow rate [m^3/h]
Q_t : sum of display value of three flowmeters [m^3/h]
S : shannon entropy [nats]
T_b : gas temperature in the buffer tank [k]
T_s : standard working temperature of flowmeter, 293 k
Δt : period of time in which mass of powder ΔW is collected in receiving hopper [h]
V_s : superficial velocity [m/s]
ΔW : mass of the powder collected in the receiving hopper for a chosen period of time Δt [kg]

Greek Letters

ρ_b : gas density in the buffer tank [kg/m^3]
ρ_c : density of powder [kg/m^3]
ρ_s : gas density at standard working condition of flowmeter (4.1×10^6 Pa, 293 K) [kg/m^3]
μ : solid-gas ratio [kg/m^3]

REFERENCES

1. A. Cowel, D. McGlinchey and R. Ansell, *Fuel*, **84**, 2256 (2005).
2. C. Liang, X. P. Chen and P. Xu, *Exp. Therm. Fluid Sci.*, **35**, 1143 (2011).
3. X. P. Chen, C. Fan and C. Liang, *Korean J. Chem. Eng.*, **24**, 499 (2007).
4. W. Pu, C. S. Zhao and Y. Q. Xiong, *Chem. Eng. Technol.*, **31**, 215 (2008).
5. J. B. Pahk and G. E. Klinzing, *J. Chin. Inst. Chem. Eng.*, **39**, 143 (2008).
6. S. Laouar and Y. Molodtsof, *Powder Technol.*, **95**, 165 (1998).
7. J. Dai and J. R. Grace, *Int. J. Multiphas Flow*, **36**, 78 (2010).
8. M. O. Carpinlioglu and M. Y. Gundogdu, *Powder Handle Process*, **12**, 145 (2000).
9. C. L. Clementson, K. E. Ileleji, *Bioresour. Technol.*, **101**, 5459 (2010).
10. J. Schaaf, J. R. Ommen and F. Taken, *Chem. Eng. Sci.*, **59**, 1829 (2004).
11. W. Zhong and M. Zhang, *Powder Technol.*, **152**, 52 (2005).
12. J. M. Hay, B. H. Nelson and C. L. Briens, *Chem. Eng. Sci.*, **50**, 373 (1995).
13. N. Ellis, L. A. Briens and J. R Grace, *Chem. Eng. J.*, **96**, 105 (2003).
14. H. Li, *Powder Technol.*, **125**, 61 (2002).
15. H. Wu, F. Zhou and Y. Wu, *Int. J. Multiphase Flow*, **27**, 459 (2001).
16. Y. J. Cho, S. J. Kim and S. H. Nam, *Chem. Eng. Sci.*, **56**, 6107 (2001).
17. W. Zhong and M. Zhang, *Powder Technol.*, **152**, 52 (2005).
18. C. Liang, C. S. Zhao and X. P. Chen, *Chem. Eng. Technol.*, **30**, 926 (2007).
19. C. Liang, X. P. Chen and C. S. Zhao, *Korean J. Chem. Eng.*, **26**, 867 (2009).
20. C. Liang, P. Xu and X. P. Chen, *Exp. Therm. Fluid Sci.*, **41**, 149 (2012).
21. D. Y. Yang, Southeast University (2008).
22. L. M. Hyder, M. S. Bradley and A. R. Reed, *Powder Technol.*, **112**, 235 (2000).